

Optical aberrations of intraocular lenses measured *in vivo* and *in vitro*

Sergio Barbero and Susana Marcos

Instituto de Óptica, Consejo Superior de Investigaciones Científicas, Calle Serrano 121, 28006 Madrid, Spain

Ignacio Jiménez-Alfaro

Fundación Jiménez Díaz, Avenida Reyes Católicos 2, 28040 Madrid, Spain

Received November 26, 2002; revised manuscript received May 14, 2003; accepted May 28, 2003

Corneal and ocular aberrations were measured in a group of eyes before and after cataract surgery with spherical intraocular lens (IOL) implantation by use of well-tested techniques developed in our laboratory. By subtraction of corneal from total aberration maps, we also estimated the optical quality of the intraocular lens *in vivo*. We found that aberrations in pseudophakic eyes are not significantly different from aberrations in eyes before cataract surgery or from previously reported aberrations in healthy eyes of the same age. However, aberrations in pseudophakic eyes are significantly higher than in young eyes. We found a slight increase of corneal aberrations after surgery. The aberrations of the IOL and the lack of balance of the corneal spherical aberrations by the spherical aberrations of the intraocular lens also degraded the optical quality in pseudophakic eyes. We also measured the aberrations of the IOL *in vitro*, using an eye cell model, and simulated the aberrations of the IOL on the basis of the IOL's physical parameters. We found a good agreement among *in vivo*, *in vitro*, and simulated measures of spherical aberration: Unlike the spherical aberration of the young crystalline lens, which tends to be negative, the spherical aberration of the IOL is positive and increases with lens power. Computer simulations and *in vitro* measurements show that tilts and decentrations might be contributors to the increased third-order aberrations *in vivo* in comparison with *in vitro* measurements. © 2003 Optical Society of America

OCIS codes: 330.0330, 170.1460, 110.3000, 080.1010, 080.3620, 170.4580.

1. INTRODUCTION

At present, surgery is the only treatment for cataract. Virtually all cataract procedures replace the natural crystalline lens with an intraocular lens (IOL). Cataract extraction with subsequent IOL implantation has evolved over the years toward less invasive procedures (smaller incisions, no sutures, etc.). The old extracapsular technique (common in the 1980s) required 14–12-mm corneal incisions and multiple sutures to seal the eye after surgery, typically resulting in an increase in astigmatism. Phacoemulsification was developed in the search for a way to extract cataracts through a smaller incision, and it has become the preferred technique for cataract extraction. An ultrasound or laser probe is used to break the lens apart, maintaining the capsule intact. The fragments are then aspirated out of the eye. A foldable IOL is then introduced through the 3–4-mm incision. Once inside the eye, the lens unfolds to take position inside the capsule. No sutures are needed, as the incision is self-sealing. Parallel to the development of surgical procedures, new IOLs have been designed with better optical surfaces and haptic shapes, new lens materials have been developed that minimize the loss of endothelial cells and the risk of capsule opacification, and new designs have been created for lens positioning during surgery.¹

IOL manufacturers and researchers have developed several methods to evaluate *in vitro* the IOL's optical quality. The most important are interferometric methods, modulation transfer function (MTF) measurements,

and resolution methods.^{2–4} Efforts have been made to standardize optical quality specifications to compare different designs and manufacturers: (American National Standard for Ophthalmics—Intraocular Lenses, and International Organization for Standardization (ISO) 11979-2 Ophthalmics Implants—Intraocular Lenses, Part 2: Optical Properties and Test Methods). Useful insight can be obtained by using aberration theory⁵ and with the help of optical simulations that use eye models. Of particular importance are the studies by Atchison^{6–8} and Lu and Smith,⁹ who evaluated theoretically the effect on optical quality of different IOL designs. These studies predict the amount of spherical aberration associated with IOLs of different shapes.

Few studies in the literature report *in vivo* objective measurements of the optical quality of eyes implanted with IOLs. Most of them measure the ocular MTF^{10–12} with double-pass techniques.¹³ These studies conclude that eyes implanted with IOLs have lower MTFs (more-degraded optics) than young eyes. In addition, monofocal IOLs produce better optical performance than diffractive multifocal IOLs. Double-pass measurements of the MTF have proved valuable and accurate, and in addition to accounting for the contribution of aberrations, they account for the degradation caused by scattering. However, the wave aberration produces a more complete description of optical quality, since it contains phase information and the sources of optical blur can be better discriminated.

To our knowledge, only a study by Mierdel *et al.*¹⁴ has

measured ocular aberrations after cataract surgery and IOL implantation (using the Tscherning's aberroscope¹⁵). However, the results are not very conclusive. Mierdel *et al.* did not find that aberrations were significantly higher in eyes after surgery than in a group of emmetropic eyes, although higher variability in postoperative data suggested some abnormalities. Other authors have studied corneal aberration changes due to the incision, but the results are controversial. Hayashi *et al.*¹⁶ found significant changes in corneal aberrations after surgery (phacoemulsification with incision length ranging from 3.5 to 6.5 mm), whereas Guirao *et al.*¹² found no significant differences between postoperative corneal aberrations (extracapsular cataract extraction with 6-mm incision) and corneal aberrations in an aged-matched group. Previous studies looking at corneal topography or keratometry limited their analyses to corneal astigmatism, most of them comparing the amount of postoperative corneal astigmatism with different localization,^{17,18} length,¹⁹ and architecture of the incision.²⁰ In the present study we combined measurements of total (using a laser ray-tracing technique^{21,22}) and corneal aberrations (using a videokeratoscope and custom software^{23–25}) in eyes that have undergone cataract surgery, and we examined the sources of aberrations in these eyes. It is well known that optical aberrations increase with age,^{26,27} mainly as a result of the shift of spherical aberration of the crystalline lens toward positive values.^{28,29} We show that replacement of the crystalline lens by a spherical IOL does not decrease the amount of aberration in elderly eyes.

Changes in corneal aberrations allow the study of possible degradation resulting from the incision. Subtracting the corneal aberrations from the total aberrations provide, we believe for the first time, measurements of the optical aberrations of the IOL *in vivo*. We also measured the aberrations of the IOL in an optical bench, using the laser ray-tracing technique and a model eye built for this purpose. Direct comparison of the aberrations of the IOL measured *in vivo* and *in vitro* allowed us to separate the optical degradation produced by the lens itself from that which may be caused by positioning errors. Finally, we performed optical simulations, using the proprietary designs provided to us by the manufacturer and computer eye models, to compare the predicted with the real optical quality.

2. METHODS

A. *In Vivo* Measurements

Total wave aberrations were measured with a laser ray-tracing technique, which has been described in detail elsewhere.^{30,31} In this technique, a laser beam samples the pupil sequentially while the corresponding aerial images of light reflected off the retina are captured on a CCD camera. The centroids of these aerial images are proportional to the derivatives of the wave aberration. The wave aberration is reconstructed by using a modal fitting to a Zernike polynomial expansion (up to 35 Zernike terms). The Zernike polynomial notation followed the recommendations of the OSA Standard Committee.³² Pupil dilatation was achieved with one drop of Tropicamide 1%. Pupil diameters in our old sub-

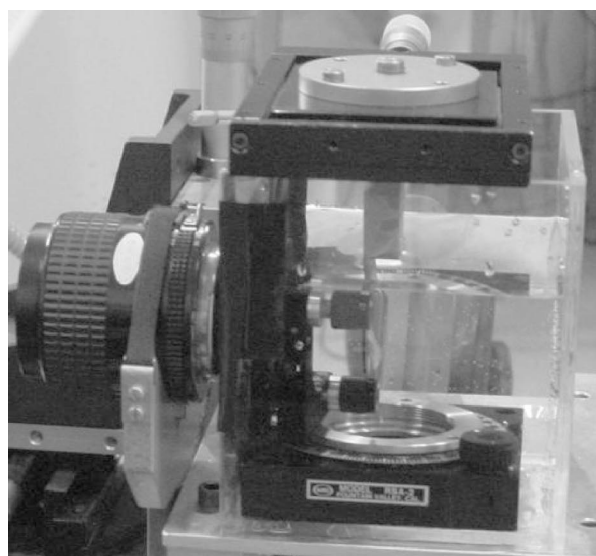
jects ranged from 5 to 6 mm (as opposed to young subjects, for whom we typically use 6.5 mm). The number of sample points in the pupil was 37 in all cases; therefore the step size ranged from 0.7 to 0.8 mm. To facilitate comparisons across subjects, all data are presented for a 5-mm pupil diameter. The pupil was continuously monitored with an IR camera. The line of sight was used in all measurements. The illumination source was a fiber-coupled near-infrared laser diode (786 nm).³³ Maximum energy exposure was 95 μW , at least one order of magnitude below safety levels prescribed by the American National Standard Institute for this wavelength.³⁴

Wave aberrations of the anterior corneal surface were obtained by virtual ray tracing with an optical design program (Zemax, October 17, 2002, Focus Software, Tucson, Ariz.). Corneal elevation maps were obtained by using a videokeratographer (Humphrey Instruments, San Leandro, Calif.). A detailed description of the procedure, computations, and validation of the technique has been presented elsewhere.^{23,25,35} The discrete height data are interpolated and transformed to Cartesian coordinates by using algorithms written in Matlab (MathWorks, Natick, Mass). The height data and their partial derivatives are used in Zemax to perform a computer ray tracing with Snell's law and to obtain the corneal wave aberration.²³ We used a realignment algorithm to ensure proper registration of the total-aberration map (measured with respect to the line of sight) and the corneal-aberration map (measured with respect to the videokeratographer).^{23–25}

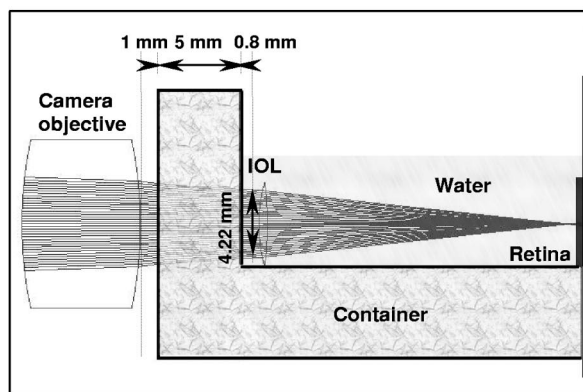
Internal aberrations were calculated by subtracting corneal aberrations from total aberrations. Internal aberrations include contributions of the crystalline lens (or the IOL) and the posterior corneal surface. In normal subjects posterior corneal contribution can be considered negligible.^{35,36} We quantified this contribution at 2% at most [root mean square (RMS) third order and higher] in an aphakic eye.³⁵

B. *In Vitro* Measurements

The aberrations of the IOL were also measured in an optical bench by using the laser ray-tracing technique. The IOL was mounted following standard methods described in the literature^{3,4,37} for MTF measurements. For this purpose, we built an eye cell model that was mounted in place of the eye in front of the laser ray-tracing technique system. Figure 1(a) shows a photograph of the eye cell model and Fig. 1(b) a schematic diagram. The eye cell model consisted of a 28-mm Nikon camera objective, which acted as the cornea (RMS = 0.18 μm). This lens produced the appropriate convergence onto the IOL. The IOL was placed in a container with 5-mm-thick methacrylate walls, filled in with water. The IOL was mounted on both x - y linear and rotational micrometer stages, to ensure proper centration and simulate positioning tilts. Simulations using Zemax were used to assess the appropriate distances and validity of the parameters used in this eye cell model. Using the Herzberger dispersion formula³⁸ for 786 nm, we computed that the error in the wave aberration measurement due to the differences in the refractive index of water (1.3309) and of the aqueous (1.3315) and the vitreous (1.3311) humors was negligible (0.003 μm). The distance between the camera objective



(a)



(b)

Fig. 1. (a) Photograph of the eye cell model system used for *in vitro* measurements. (b) Schematic diagram of the eye cell model, consisting of a camera objective, a methacrylate cube filled with water, the IOL mounted on a rotation stage, and an artificial retina.

and the IOL was set so that the convergence of rays on the IOL was equivalent to that of the real eye. A convergence angle of 5.1 deg (which we computed in Zemax for the postoperative cornea of eye #7) was achieved by placing the IOL 6.08 mm behind the camera lens (and 0.8 mm from the wall of the water container). We also computed the appropriate sampling-pattern diameter to achieve an effective IOL aperture similar to the diameters measured in real eyes. For a distance of 4.2 mm between the posterior corneal surface and the IOL (measured by optical biometry for eye #11) and a 5-mm sampled pupil, the effective aperture on the IOL is 4.22 mm, achieved by using a 5-mm pupil in the eye model. Since the measurements were done in a double-pass configuration, a diffuser surface was placed at the focal plane, acting as the retina. In order to avoid speckle noise in the aerial images, we increased normal exposure times (100 ms) to 300 ms while the diffuser was moved vertically. Eliminating the speckle in the images is necessary to ensure accurate de-

tection of the centroids. As in the real eye, we obtained sets of 37 aerial images, from which the wave aberration was computed.

To eliminate aberrations introduced by the camera lens, and especially the spherical aberration introduced by the container (RMS = 0.09 μm), we obtained a reference set of data with the IOL removed. The aberrations of the IOL (directly comparable to the internal aberrations in the eye) were computed by subtraction of this reference from the total aberrations, since the wave aberrations through different elements are additive.

C. Computer Modeling

We performed computer simulations by using an optical design program (Zemax) to evaluate the theoretical optical performance of the IOLs. We estimated the IOL wave aberration and spherical aberration (in terms of Z_4^0) for a model cornea as a function of IOL power, as well as individual predictions of total spherical aberration by using individual corneal topography, anterior chamber depth, and IOL parameters. This modeling also allowed us to test the effects of IOL tilt and decentration. The computer simulations were performed with use of monochromatic ray tracing (786 nm). Data from anterior radius, posterior radius, and thickness of IOLs similar to those tested in this study, as well as refraction index (1.55) were provided to us by the manufacturer. All lenses were bi-convex (spherical surfaces) except for the 0-D (diopter) lens, which was a meniscus.

For comparison with *in vitro* measurements, converging rays with the same angle and the same effective pupil as in the eye cell model were traced through the IOL. For comparison with *in vivo* measurements, the individual corneal elevation maps and anterior chamber depths were used. The posterior corneal surface was simulated as an aspheric surface of 6.31-mm radius and -0.51 asphericity (asphericity = $-e^2$, where e is the conic eccentricity); these values were taken from experimental values for aging corneas.³⁹ Corneal refraction index was assumed 1.371 (for 786 nm), and corneal thickness was assumed 0.5 mm. Estimates were obtained on the optical axis (i.e., shift of the fovea from the optical axis was not taken into account) and for the pupil centered on the optical axis.

D. Modulation-Transfer-Function Calculations

We computed the MTF, i.e., the modulus of the optical transfer function, from the wave aberration by using Fourier optics and routines written in Matlab. The MTF is the modulus of the autocorrelation of the pupil function, where the pupil function is

$$P(\alpha, \beta) = T(\alpha, \beta) \exp \left[-i \frac{2\pi}{\lambda} W(\alpha, \beta) \right],$$

where W is the wave aberration and T is the pupil transmittance, α and β are the pupil coordinates, and λ is the wavelength (786 nm). We ignored pupil apodization by the Stiles-Crawford effect, i.e., $T(\alpha, \beta) = 1$. The MTF was calculated from the ocular wave aberrations measured *in vivo* and from *in vitro* and simulated IOL wave aberrations. In all the computations, only third- and

higher-order aberrations were considered (i.e., defocus and astigmatism were set to zero).

E. Subjects

We measured total and corneal aberrations in nine eyes from seven subjects (mean age 70.6 ± 9 yr.) after cataract surgery. The two types of measurement were conducted in the same experimental session, at least two months after surgery. Axial length and anterior chamber depth by optical biometry (IOLMaster, Humphrey-Zeiss) and autorefractometry (Automatic Refractor Model 597, Humphrey-Zeiss) were also obtained in each session. Table 1 provides preoperative and postoperative values of the eyes under test. Some of these patients were also available before surgery. We measured total aberrations in six of these eyes and corneal aberrations in two of these eyes before surgery. Postoperative corneal aberrations were also measured in an eye (#16) that was not available for total-aberration measurements.

All the surgeries were performed by the same surgeon using a phacoemulsification technique, with a 4.1-mm superior corneal incision (except in eye #16, which had a 3-mm superior limbal incision) made by a calibrated blade. No posterior suture was necessary. The implanted IOLs were 5.5-mm monofocal foldable lenses, with powers ranging from 0 to 26 D (mean 19.43 D). Table 1 shows the corresponding power for each subject. Four equivalent IOLs (0, 12, 16, and 23 D) were measured in an optical bench with the laser ray-tracing technique, as described above.

Comparisons of total and corneal aberrations were also made with respect to a group of nearly emmetropic (<4 D) and young (29 ± 3.7 yr.) eyes that were available from previous studies in which the same instruments had been used.

The study followed the tenets of the Declaration of Helsinki. Subjects were appropriately informed about the

nature of the study and signed an informed-consent form approved by the Institutional Ethical Committees.

3. RESULTS

A. *In Vivo* Measurements

Figure 2(a) shows postoperative total, corneal, and internal wave aberration maps in all eyes measured. Tilts and defocus have been canceled. For each eye the same gray scale has been used for all three maps but has been changed across subjects. All internal wave aberration maps (excluding also astigmatism) with the same scale are represented in Fig. 2(b). Contours are plotted at $1\text{-}\mu\text{m}$ intervals in all maps. A great inter-eye variability is observed. In some eyes (i.e., eyes #9 and #10) the aberrations of the IOL seem to contribute more than those of the cornea to total wave aberration, while in other eyes (i.e., eye #8), the aberrations of the cornea dominate. In the remaining eyes both corneal and IOL aberrations contribute significantly. The peak-to-valley range was from $\pm 3\ \mu\text{m}$ in most internal third- and higher-order aberration patterns [see Fig. 2(b)], indicating an important contribution of IOL aberrations *in vivo*.

Figure 3 shows changes in corneal RMS for the three eyes measured before and after surgery. Third- and higher-order aberrations increase in all three eyes, particularly in eye #16. Astigmatism increases in eyes #14 and #16 but not in eye #8, where it decreases from 1.18 to 0.17 D.

Figure 4 compares mean third- and higher-order RMS in pseudophakic eyes with respect to the group of 6 preoperative eyes (mean age 70 ± 10.55 yr.) and a group of 14 young, nearly emmetropic eyes (mean age 29 ± 3.7 yr.). The amount of aberrations after cataract surgery (RMS = $0.62 \pm 0.18\ \mu\text{m}$) is not significantly different ($p = 0.93$) from that in old eyes before cataract surgery (RMS = $0.61 \pm 0.24\ \mu\text{m}$), and it is 3.02 times

Table 1. Subjects' Measurements

Subject	Eye #	OD/OS	Age	Refraction	Axial Length (mm)	Anterior Chamber Depth (mm)	IOL Power (D)
Preoperative Eyes							
A	1	OS	51	$-7.00 + 0.25 \times 58$	25.31	2.32	—
B	2	OD	67	$-3.25 + 0.75 \times 107$	26.43	3.46	—
C	3	OD	81	$-2.25 + 1.25 \times 3$	23.42	3.09	—
D	4	OD	77	$-1.75 + 0.5 \times 180$	22.47	2.64	—
F	5	OS	74	$+2.00 + 0.75 \times 17$	22.37	3.78	—
F	6	OD	74	$+2.00 + 0.75 \times 162$	22.47	3.11	—
Postoperative Eyes							
A	7	OD	51	$-1.75 + 0.00 \times 180$	30.33	4.47	0
A	8	OS	51	$-3.50 + 1.25 \times 175$	25.16	2.54	14
B	9	OS	67	$-2.00 + 1.00 \times 13$	26.07	4.94	16.5
C	10	OS	81	$-1.50 + 0.5 \times 16$	23.20	2.91	21
D	11	OS	77	$-3.00 + 3.00 \times 18$	22.46	4.2	23
E	12	OD	72	$-0.25 + 0.50 \times 12$	22.66	3.98	23
E	13	OS	72	$-1.50 + 0.5 \times 169$	22.36	4.27	23
F	14	OS	74	$-1.75 + 0.75 \times 4$	22.29	4.33	25.5
G	15	OD	72	$-1.25 + 0.25 \times 58$	22.01	3.19	26
H	16	OS	71	$-2.50 + 3.00 \times 172$	25.19	5.11	—

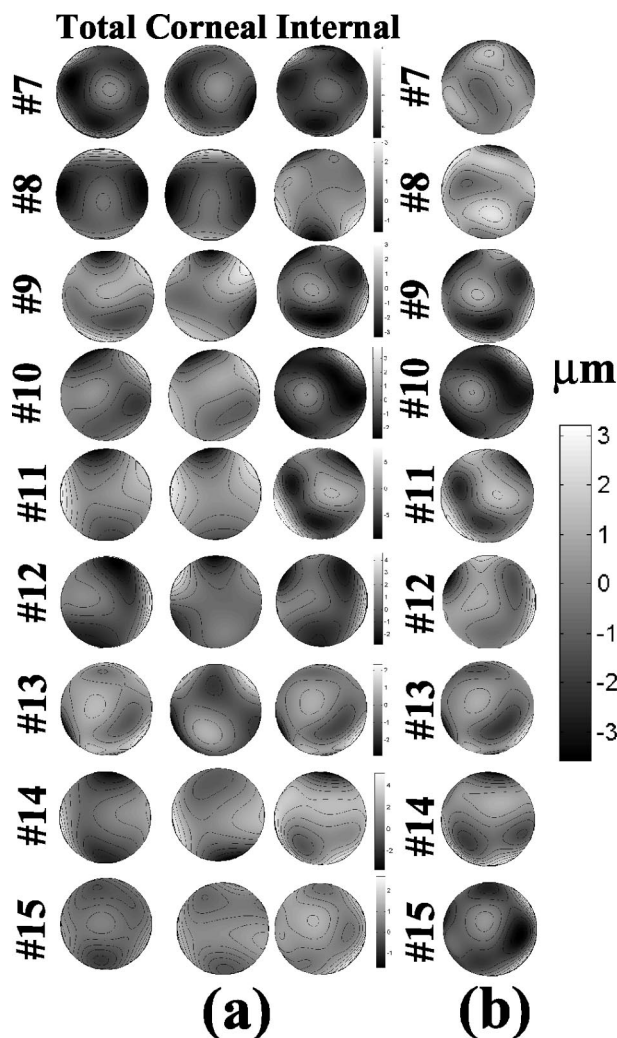


Fig. 2. (a) Wave aberration patterns (without tilts and defocus) of nine postcataract-surgery eyes, measured *in vivo*, for total aberrations (first column), corneal aberrations (middle column) and internal aberrations (third column). Contour lines are plotted every 1 μm . The gray-scale bar represents wave aberration heights in micrometers. The same scale was used for all eyes. Diameters were 5 mm. (b) Internal wave aberration patterns (excluding astigmatism) for all eyes, plotted on a common scale.

higher than in young eyes. Postoperative corneal aberrations are slightly worse (RMS = $0.54 \pm 0.27 \mu\text{m}$) than, but not statistically significant ($p = 0.24$) from, the preoperative values (RMS = $0.41 \pm 0.08 \mu\text{m}$) and are significantly worse ($p = 0.0003$) than in young eyes (RMS = $0.23 \pm 0.1 \mu\text{m}$). The aberrations of our preoperative group are similar to aberrations of healthy eyes of the same age group reported in previous studies: for total aberrations, RMS = $0.7 \mu\text{m}$ for a 6-mm pupil, from Artal *et al.*⁴⁰; and RMS = $1.1 \mu\text{m}$, for a 7.32-mm pupil, from McLellan *et al.*²⁶; for corneal aberrations, RMS = $0.5 \mu\text{m}$ for a 6-mm pupil from Artal *et al.*⁴⁰ Therefore this comparison could be extrapolated to a wider population.

B. In Vitro Measurements

The IOL wave aberrations of the four IOLs measured *in vitro* are shown in Fig. 5, excluding tilts and defocus. All

aberrations represented on the same scale. As for measurements *in vivo*, the amount of aberrations is significantly different from zero. The mean that the RMS of IOLs (excluding tilt and defocus) is $0.49 \pm 0.23 \mu\text{m}$ (as opposed to $0.47 \pm 0.3 \mu\text{m}$ for young lenses), while the RMS for third- and higher-order aberrations is $0.34 \pm 0.01 \mu\text{m}$, slightly larger than in young lenses ($0.25 \pm 0.15 \mu\text{m}$). This means that a higher amount of astigmatism is found in natural crystalline lenses than in the IOLs measured *in vitro*, but the IOLs show a higher amount of third- and higher-order aberrations.

C. Comparison of Measurements *in Vivo* and *in Vitro* with Estimations from Simulations

Figure 6 shows RMS values for measurements of IOL *in vivo* and *in vitro*. Third- and higher-order RMS is significantly greater (2.48 times) measured *in vivo* than measured *in vitro* ($p = 0.015$).

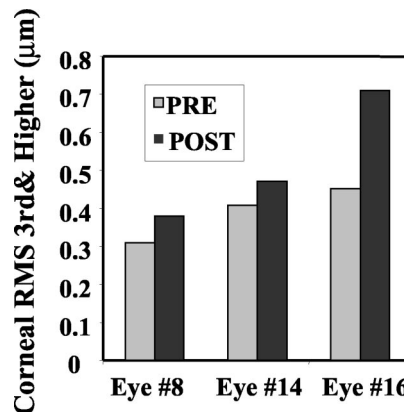


Fig. 3. Corneal RMS wave-front error for third- and higher-order aberrations, preoperative (gray bars) and postoperative (black bars), for eyes #8, #14, and #16.

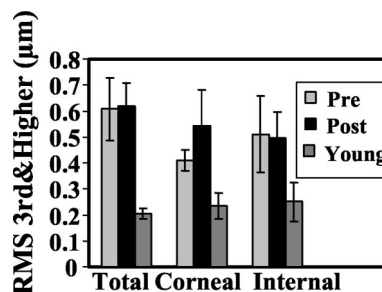


Fig. 4. Average total, corneal, and internal RMSs (third- and higher-order aberrations) for preoperative (light-gray bars), postoperative (black bars), and young eyes (dark-gray bars). Error bars represent standard deviation.

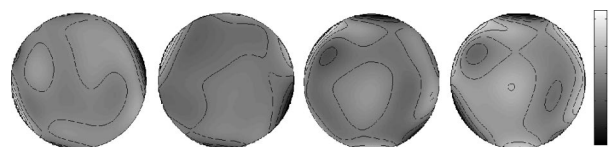


Fig. 5. Wave aberration patterns (third- and higher-order aberrations) of IOLs measured *in vitro*, with use of the eye cell model depicted in Fig. 1 and the laser ray-tracing technique.

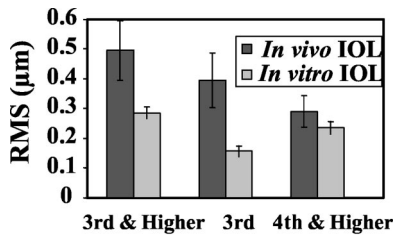


Fig. 6. Comparison of average IOL RMS *in vivo* (black bars) and *in vitro* (gray bars), for third- and higher-order, third-order, and fourth- and higher-order aberrations and astigmatism.

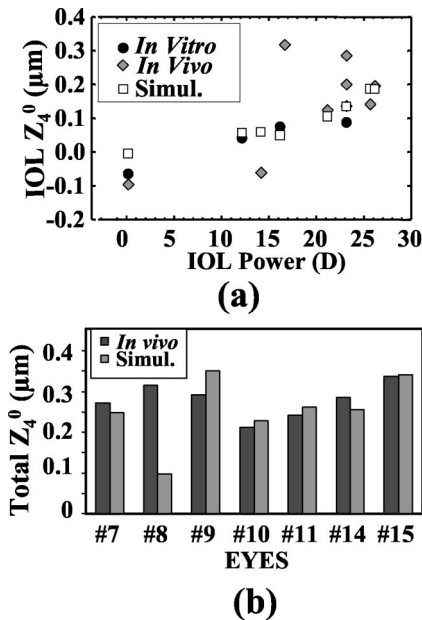


Fig. 7. (a) Spherical aberration (Z_4^0) of the IOLs as a function of IOL power, from *in vivo* measurements (diamonds), *in vitro* measurements (circles), and simulations (squares). (b) Total spherical aberration (Z_4^0), from *in vivo* experimental measurements (black bars), and simulations (gray bars) with use of ocular individual parameters (corneal topography, lens position, axial length) and the corresponding IOL parameters.

Fourth- and higher-order RMS is not significantly different ($p = 0.35$) in the two types of measurements. The main contribution to aberrations measured *in vitro* comes from fourth- and higher-order aberrations, whereas the main contribution *in vivo* comes from third-order aberrations. Also, there is a larger variability *in vivo* ($0.24 \mu\text{m}$) than *in vitro* ($0.09 \mu\text{m}$) across IOL measurements.

Figure 7(a) shows the spherical aberration (Z_4^0) of the IOL from *in vivo* and *in vitro* measurements and from simulations as a function of IOL power. There is an increase toward more positive values of spherical aberration with IOL power. The trend is similar in all types of measures, which indicates that the largest contribution to this effect is associated with the IOL. Except for 0 D (and one exceptional measurement *in vivo*), all values of spherical aberration are positive: $0.17 \pm 0.12 \mu\text{m}$ for *in vivo* measurements, $0.07 \pm 0.02 \mu\text{m}$ for *in vitro* measurements, and $0.11 \pm 0.06 \mu\text{m}$ for simulations). The spherical aberration of the natural crystalline lens in our young group is $-0.01 \pm 0.09 \mu\text{m}$.

Simulations of IOL aberrations on axis produced only spherical aberration, owing to the rotational symmetry of the design. Simulated tilts and decentrations of the lenses produced coma and astigmatism and are discussed in Section 4.

Figure 7(b) compares total spherical aberration measured with the laser ray-tracing technique *in vivo* and simulations using eye models. These models include individual data of anterior corneal elevation, anterior chamber depth, and IOL design. There is a good agreement between experimental measurements and simulations from custom eye models, except for one lens (14 D).

4. DISCUSSION

A. Limitations of the Measurements

The laser ray-tracing technique proved very efficient for measuring aberrations in elderly patients after surgery, and even before surgery in some patients. The facts that in this technique the aerial images are captured sequentially and that a large area of the CCD is available for each image allow more optical degradation (caused by aberrations or scattering) than other conventional techniques such as the Shack-Hartmann. Aerial retinal images through cataracts were typically more spread out and noisy than in normal eyes, owing to an increase in intraocular opacity and scattering.⁴¹ In several cases the spot diagram (set of centroids computed from the aerial images) showed rather inhomogeneous patterns that were probably due to large deviations of the rays produced by local lens opacities. We checked the continuity of the spot diagrams by comparing the experimental spot diagram with that derived from the computed wave aberration. Four eyes out of the ten measured before cataract surgery were excluded because of a lack of correspondence of computed and simulated spot diagrams. Aerial retinal images from postoperative eyes typically showed larger halos than those from normal eyes. This is probably due to the higher reflectivity of the IOL surfaces⁴² caused by their higher index of refraction (1.55, versus less than 1.395 in the natural lens⁴³). Centration and head stability of the subjects during measurement were also typically poorer in elderly patients than in normal young subjects. As a result of the above, variability was slightly larger in these measurements than in previous studies in young subjects. The Zernike coefficient standard deviation (averaged across terms) was $0.1 \pm 0.03 \mu\text{m}$ and $0.18 \pm 0.19 \mu\text{m}$ preoperative and postoperative, respectively, while for the young reference group the standard deviation was $0.05 \pm 0.02 \mu\text{m}$.

B. Sources of Aberrations after Cataract Surgery

1. Corneal Aberrations

Our analysis of preoperative and postoperative corneal aberrations is limited to three eyes and therefore does not have sufficient statistical power. However, all three corneas show an increase in third- and higher-order RMS: 0.07, 0.06, and $0.26 \mu\text{m}$ in eyes #8, #14, and #16, respectively. It has been reported, although to a much lesser extent than in previous techniques requiring a suture, that the small incision in phacoemulsification induces slight changes in astigmatism. Our results suggest that

higher-order aberrations are also modified and tend to increase (see Fig. 3). The incision was performed in the vertical meridian and superior in these eyes. Incision on the steepest meridian has been reported to produce a relaxation of this meridian, therefore avoiding postoperative astigmatism, for preoperative astigmatism of 0.5 D or higher.⁴⁴ Preoperative corneal astigmatic axis was against the rule (2.3 and 172.1°) in eyes #14 and #16, respectively. In these eyes the incision was made in the flattest meridian instead of the steepest, which resulted in an increase of astigmatism. Preoperative astigmatism was with the rule (88.6°) in eye #8, and as expected, astigmatism decreased after surgery.

2. Aberrations of the Intra-Ocular Lens

Measurements *in vivo* and *in vitro* show that positive spherical aberration is present in IOLs and increases with IOL power. Comparison with computer simulations shows that the spherical design of the IOL surfaces results in the observed positive spherical aberration. These results agree with previous predictions by Atchison *et al.*⁷ Fifth- and higher-order terms are present in both *in vivo* and *in vitro* measurements but not in results from computer simulations (based on IOLs with purely spherical surfaces).

3. Tilt and Decentration of the Intra-Ocular Lens

Except for the spherical aberration, the *in vivo* IOL aberrations are higher in most terms (particularly third-order aberrations) than the equivalent aberrations measured *in vitro*.

Several studies in the literature report tilts and decentrations of different types of pseudophakic IOLs based on measurements with use of Purkinje images or Scheimpflug lamp biomicroscopy. Using Purkinje images, Philips *et al.*,⁴² reported average tilt values of 7.8 deg and 0.7 mm of decentration.⁴² Mutlu *et al.*⁴⁵ reported lower values: mean tilt of 2.83 deg and mean decentration of 0.28 mm. Jung *et al.*⁴⁶ reported tilts of up to 3.01 deg (mean tilt of 2.35 deg) measured with use of a Scheimpflug lamp.

Our study has not directly measured the tilts and decentration of IOLs *in vivo*. Using the eye cell model and computer simulations, we evaluated the effect of plausible IOL tilts and decentrations on the aberration pattern. Figure 8(a) shows results of RMS (for third- and higher-order aberrations) for an IOL of 16 D for centered and tilted positions of 4 and -4 deg respectively. Tilts were achieved by physically rotating the lens by using a micrometer stage within the cell or by computationally ro-

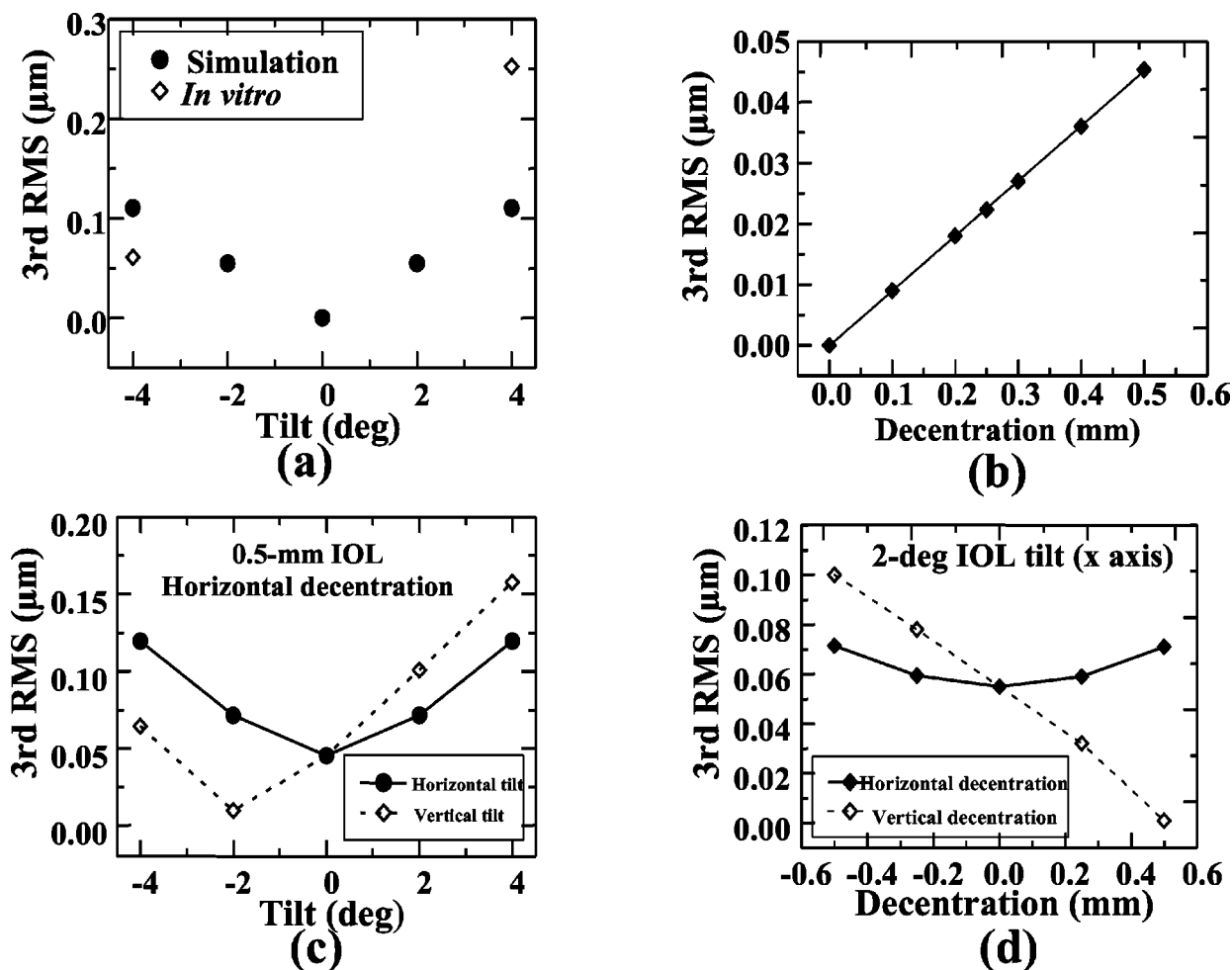


Fig. 8. (a) Changes in third-order IOL RMS as a function of tilt from *in vitro* measurements (open diamonds) and from simulations (solid circles). (b) Simulated IOL third-order RMS as a function of lens decentration. (c) Simulated third-order IOL RMS as a function of lens horizontal and vertical tilts, for a fixed simulated 0.5-mm IOL horizontal decentration. (d) Simulated third-order IOL RMS as a function of horizontal and vertical decentrations of the IOL, for a fixed simulated 2-deg IOL tilt (horizontal axis).

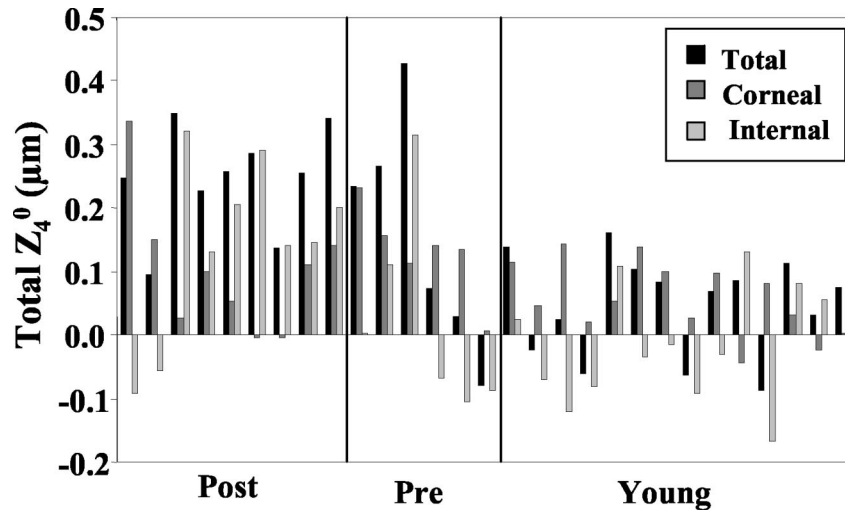


Fig. 9. Total (black bars), corneal (dark-gray bars), and internal (light-gray bars) spherical aberration (Z_4^0) for young, preoperative, and postoperative eyes.

tating the lens about the horizontal axis. Third-order RMS increased on average by $0.15 \mu\text{m}$ with respect to the centered position for a tilt of 4 deg, comparable to results from the simulations ($0.10 \mu\text{m}$) [see Fig. 8(a)]. Results from simulations show that third-order RMS increases linearly with IOL decentration and by $0.045 \mu\text{m}$ for 0.5-mm decentration [Fig. 8(b)]. Combined tilt and decentration are most likely present in real eyes. No particular trend has been reported in the literature for the direction of decentration.^{42,47} Tilts seem more predominant along the horizontal or the vertical axis.⁴² We tested the effect of various tilts for a certain amount of decentration (0.5 mm), Fig. 8(c), and the effects of various amounts of decentrations for a given tilt, Fig. 8(d). Our simulations show that some specific combinations of tilt and decentration may counteract the introduction of third-order aberrations, while other combinations add up the effect [Figs. 8(b) and 8(c)], indicating that the correlation between tilts/decenterations and third-order aberrations present in real eyes implanted with IOLs can be complex. Experimental measurements of tilts and decentrations in each individual eye are necessary to quantify their actual effect on third-order aberrations measured in each eye.

4. Lack of Balance between Corneal and Internal Aberrations

The increase of the total aberrations with age in our study is in agreement with some studies reported previously in the literature.²⁶ This can be due to two factors: (1) The increase of corneal and lenticular aberrations. The old/young RMS ratio is 2.04 for internal aberrations and 1.75 for corneal aberrations. (2) A certain degree of loss of balance between corneal and internal aberrations (as found by Artal *et al.*⁴⁰). Total RMS in young eyes is lower than corneal RMS, whereas in old eyes total RMS is 1.48 higher than corneal RMS.

It seems widely accepted that the natural crystalline lens corrects to some extent the aberrations of the cornea, particularly the spherical aberration. Artal *et al.*^{12,40} suggested that this balance was disrupted with aging. A

reasonable explanation is that with aging, the spherical aberration of the crystalline lens shifts toward more positive values, as reported by *in vivo*²⁹ and *in vitro* studies.⁴⁸ Our data show that the spherical aberration of the IOL is positive, as opposed to negative in young eyes [see Fig. 7(a) and Fig. 9]. It is therefore expected that, as found in old natural eyes, a lack of balance between corneal and internal spherical aberration is also responsible for the increased RMS in pseudophakic eyes in comparison with young eyes.

Using RMS ratios is not an optimal way to evaluate the degree of corneal-to-internal balance, because the RMS does not take into account the coefficient sign, and multiple cross-terms prevent a direct analysis. Instead, we performed a term-by-term analysis and evaluated, for each term, the amount of corneal correction by the crystalline lens and vice versa. For each eye we defined a series of 37 compensation values (corresponding to the 37 Zernike coefficients). Compensation values (CV_i) were defined as $CV_i = \text{sign}(C_{\text{corneal}}/C_{\text{internal}}) \times \min(C_{\text{corneal}}, C_{\text{internal}})$. The rationale for this definition is as follows: The first term (sign of cornea/internal ratio) indicates presence (if negative) or absence (if positive) of compensation. If corneal and internal coefficients have different signs, then some compensation occurs, whereas if they have the same sign (positive term) they will add up. The second term is indicative of the amount of compensation. The minimum value between C_{corneal} and C_{internal} represents the amount of aberration subtracted from the aberration of the dominant component (if sign is different for C_{corneal} and C_{internal}) or the amount that adds up (if the sign is the same for C_{corneal} and C_{internal}). Therefore a high term value with a negative sign is indicative of a high degree of compensation between ocular components, whereas a high term with a positive value is indicative of an addition of the aberrations. We found a slight loss of balance in third-order terms with age (average $CV_i = -0.079 \mu\text{m}$ for young and $-0.049 \mu\text{m}$ for old eyes) but no significant difference between young and postoperative eyes ($-0.087 \mu\text{m}$). Compensation values for astigmatism and spherical aberra-

tion show important differences. Average CV_i for astigmatism is $-0.178 \mu\text{m}$ in young eyes, whereas for old and postoperative eyes it shows positive values (0.040 and $0.045 \mu\text{m}$, respectively), indicating a lack of compensation. For spherical aberration, we found negative values for young eyes ($-0.025 \mu\text{m}$), indicating compensation, and positive values in old and postoperative eyes (0.007 and $0.03 \mu\text{m}$, respectively). Figure 9 shows total, corneal, and internal spherical values (Z_4^0) for young, preoperative, and postoperative eyes.

C. Modulation Transfer Functions: *in Vivo* and *in Vitro* Measurements

All previous *in vivo* data of optical quality after cataract surgery were obtained by using a double-pass technique,¹⁰⁻¹² which can provide only the MTF. Most *in vitro* assessments of the optical quality of IOLs are based on MTF measurements.²⁻⁴ We computed MTFs from the measured wave aberrations *in vivo* (total and IOL MTF), *in vitro*, and in simulated wave aberrations (IOL MTF).

In Fig. 10 we compare total average MTF of the group of young and postoperative eyes with previous *in vivo* data reported in the literature from studies that used double-pass techniques. These previous studies measured a group of patient eyes implanted with monofocal polymethylmethacrylate (PMMA) IOLs after extracapsular cataract extraction¹² and a group with monofocal IOLs (FORMFLEX II, IOLAB),¹¹ respectively. The MTF is substantially higher for young eyes than any postoperative MTF measurement, for the entire spatial frequency range. Differences between postoperative data from our study and data from other groups are smaller than differences between our postoperative data and data in young eyes, despite the different surgical techniques and IOLs. However, our *in vivo* MTFs are significantly higher, particularly for high frequencies, than those measured previously. The fact that the surgical technique is less invasive (minimizing the impact of the incision) and possible

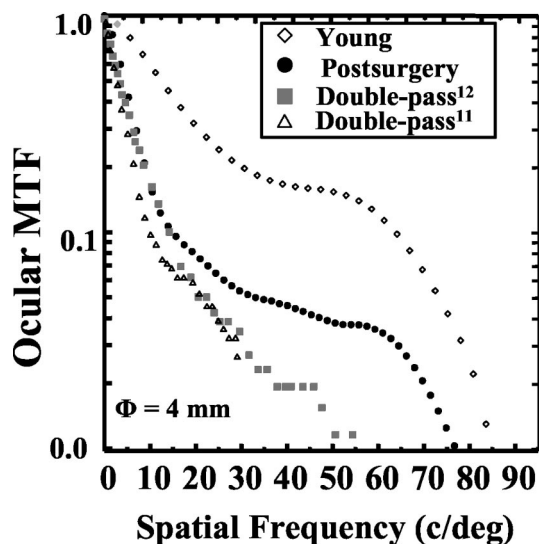


Fig. 10. Average MTF (radial profile), computed from the wave aberrations for the young and the postoperative groups in comparison with double-pass MTF measurements from previous studies by Artal *et al.*¹¹ and Guirao *et al.*¹² Pupil diameter = 4 mm.

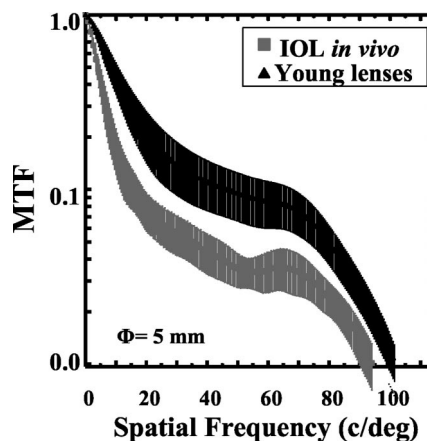


Fig. 11. Average MTF (radial profile) computed from the wave aberration for a group of young crystalline lenses and for IOLs, both measured *in vivo*. Pupil diameter = 5 mm. Error bars represent standard deviation across eyes.

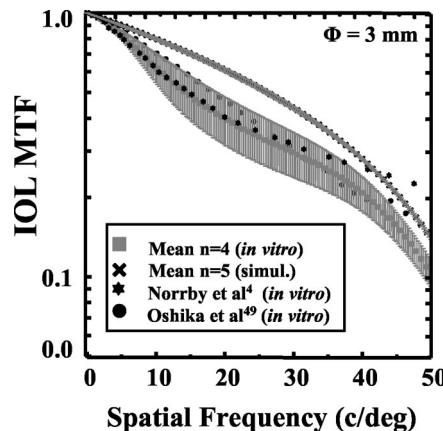


Fig. 12. Average MTF (radial profile) computed from the wave aberration for *in vitro* measurements and simulations from this study and for *in vitro* MTF measurements by Oshika and Shiokawa⁴⁹ and by Norrby *et al.*⁴ Pupil diameter = 3 mm. Error bars represent standard deviation of the *in vitro* measurements across eyes.

differences across the different types of lenses are possible reasons for the improvement. Another possible explanation is that double-pass MTFs have been found to be consistently lower than MTFs estimated from wave aberrations, because they are affected by scattering and higher-order aberrations not measured by aberrometers. The potential influence of retinal scattering in double-pass measurements in older eyes has never been studied, and therefore we cannot quantify its relative contribution to the difference.

Figure 11 shows the MTFs that are due only to internal aberrations. The optical quality of young lenses is clearly better than that of IOLs for all frequencies. Figure 12 compares MTFs of the IOL from *in vitro* measurements with previous *in vitro* measurements on acrylic IOLs⁴⁹ and PMMA IOLs.⁴ MTFs from computer ray-tracing simulations on the IOLs from our study are also included. For a proper comparison with earlier studies, we recalculated the MTF for a 3-mm-diameter aperture. Comparing our *in vivo* measurements with those of

Oshika and Shiokawa⁴⁹ and those of Norrby *et al.*,⁴ we found no significant differences except for the higher spatial frequencies beyond 35 cycles per degree (c/deg). The MTF predicted from the optical design of the IOLs of this study is significantly higher than other MTF measurements (except for frequencies beyond 40 c/deg, where PMMA *in vitro* measurements show slightly higher values). The fact that there is a consistent discrepancy between predictions and measurements on the optical bench may be indicative of some differences between theoretical designs and final lens manufacturing and experimental handling.

5. SUMMARY AND CONCLUSIONS

We summarize our findings as follows:

1. We measured, for the first time, the aberrations of IOLs *in vivo*.

2. Previous *in vivo* data were limited to MTFs measured by double-pass techniques. The use of corneal and total wave aberrations allowed us to estimate the sources of degradation of optical quality in eyes after cataract surgery.

3. Optical quality after cataract surgery is significantly lower in pseudophakic eyes (RMS for third- and higher-order terms $0.62 \pm 0.18 \mu\text{m}$) than in young eyes ($0.2 \pm 0.04 \mu\text{m}$). The amount of aberrations in pseudophakic eyes is similar to that in phakic eyes of the same age group. These conclusions are based on a small data set but show a very consistent trend and are highly statistically significant.

4. From measurements of spherical IOLs *in vivo* and *in vitro* and computer simulations, we conclude that the spherical aberration of the IOL (which is positive and increases with IOL power) is a source of optical degradation. As opposed to the case with young eyes, there is no balance of corneal and internal spherical aberrations and astigmatism.

5. The IOL's third-order aberrations measured *in vivo* are much higher ($0.4 \pm 0.18 \mu\text{m}$) than *in vitro* ($0.16 \pm 0.04 \mu\text{m}$). IOL tilts and decentrations could be responsible for this further decrease in optical quality.

6. IOL optical quality (measured both *in vivo* and *in vitro*) is lower than predicted from simulations, possibly indicating some discrepancies from the theoretical design.

7. Laser ray tracing and corneal topography are useful techniques for understanding the optical changes induced by cataract surgery. These measurements allow validation of predictions of optical quality with IOLs with use of individual eye models as well as exploration of possible new designs.

ACKNOWLEDGMENTS

The authors have no proprietary interest in the materials presented in this article. This research was funded by grants CAM 08.7/0010/2000 (Comunidad Autónoma de Madrid, Spain) and BFM2002-02638 (Ministerio de Ciencia y Tecnología, Spain) to Susana Marcos. The Consejo Superior de Investigaciones Científicas, Carl Zeiss, Spain, and Ministerio de Educación y Cultura and Residencia de

Estudiantes funded fellowships to Sergio Barbero. The manufacturer provided commercially available IOLs for *in vitro* measurements and relevant design values for computer simulations. The authors thank Jesus Merayo for his contributions in the early stages of this study and Lourdes Llorente for her help with experimental measurements and data handling.

Corresponding author Susana Marcos may be reached by e-mail at susana@io.cfmac.csic.es.

REFERENCES

1. D. T. Azar, *Intraocular Lenses in Cataract and Refractive Surgery* (Saunders, Philadelphia, Pa., 2001).
2. M. J. Simpson, "Optical quality of intraocular lenses," *J. Cataract Refractive Surg.* **18**, 86–94 (1992).
3. V. Portney, "Optical testing and inspection methodology for modern intraocular lenses," *J. Cataract Refractive Surg.* **18**, 607–613 (1992).
4. N. E. Norrby, L. W. Grossman, E. P. Geraghty, C. F. Kreiner, M. Mihori, A. S. Patel, V. Portney, and D. M. Silberman, "Determining the imaging quality of intraocular lenses," *J. Cataract Refractive Surg.* **24**, 703–714 (1998).
5. G. Smith and C. W. Lu, "The spherical aberration of intraocular lenses," *Ophthalmic Physiol. Opt.* **8**, 287–294 (1988).
6. D. Atchison, "Third-order aberrations of pseudophakic eyes," *Ophthalmic Physiol. Opt.* **9**, 205–210 (1989).
7. D. A. Atchison, "Optical design of intraocular lenses. I. On-axis performance," *Optom. Vision Sci.* **66**, 492–506 (1989).
8. D. Atchison, "Design of aspheric intraocular lenses," *Ophthalmic Physiol. Opt.* **11**, 137–146 (1991).
9. C. W. Lu and G. Smith, "Aspherizing of intra-ocular lenses," *Ophthalmic Physiol. Opt.* **10**, 54–66 (1990).
10. R. Navarro, M. Ferro, P. Artal, and I. Miranda, "Modulation transfer functions of eyes implanted with intraocular lenses," *Appl. Opt.* **32**, 6359–6367 (1993).
11. P. Artal, S. Marcos, R. Navarro, I. Miranda, and M. Ferro, "Through focus image quality of eyes implanted with monofocal and multifocal intraocular lenses," *Opt. Eng.* **34**, 772–779 (1995).
12. A. Guirao, M. Redondo, E. Geraghty, P. Piers, S. Norrby, and P. Artal, "Corneal optical aberrations and retinal image quality in patients in whom monofocal intraocular lenses were implanted," *Arch. Ophthalmol.* **120**, 1143–1151 (2002).
13. J. Santamaria, P. Artal, and J. Bescós, "Determination of the point-spread function of human eyes using a hybrid optical-digital method," *J. Opt. Soc. Am. A* **4**, 1109–1114 (1987).
14. P. Mierdel, M. Kaemmerer, H. E. Krinke, and T. Seiler, "Effects of photorefractive keratectomy and cataract surgery on ocular optical errors of higher order," *Graefes Arch. Clin. Exp. Ophthalmol.* **237**, 725–729 (1999).
15. M. Mrochen, M. Kaemmerer, P. Mierdel, H. E. Krinke, and T. Seiler, "Principles of Tscherning aberrometry," *J. Refract. Surg.* **16**, S570–S571 (2000).
16. K. Hayashi, H. Hayashi, T. Oshika, and F. Hayashi, "Fourier analysis of irregular astigmatism after implantation of 3 types of intraocular lenses," *J. Cataract Refract. Surg.* **26**, 1510–1516 (2000).
17. T. Oshika, G. Sugita, T. Tanabe, A. Tomidokoro, and S. Amano, "Regular and irregular astigmatism after superior versus temporal scleral incision cataract surgery," *Ophthalmology* **107**, 2049–2053 (2000).
18. R. Gross, "Corneal astigmatism after phacoemulsification and lens implantation through uncut scleral and corneal tunnel incisions," *Am. J. Ophthalmol.* **121**, 57–64 (1996).
19. T. Kohnen, B. Dick, and K. Jacobi, "Comparison of the induced astigmatism after temporal clear corneal tunnel inci-

- sions of different sizes," *J. Cataract Refract. Surg.* **21**, 417–424 (1995).
20. P. Nielsen, "Prospective evaluation of surgically induced astigmatism and astigmatic keratotomy effects of various self-sealing small incisions," *J. Cataract Refract. Surg.* **21**, 43–48 (1995).
 21. R. Navarro and M. A. Losada, "Aberrations and relative efficiency of light pencils in the living human eye," *Visual Opt.*, (1996).
 22. R. Navarro and E. Moreno-Barriuso, "A laser ray-tracing method for optical testing," *Opt. Lett.* **24**, 951–953 (1999).
 23. S. Barbero, S. Marcos, J. Merayo-Llodes, and E. Moreno-Barriuso, "Validation of the estimation of corneal aberrations from videokeratography in keratoconus," *J. Refract. Surg.* **18**, 263–270 (2002).
 24. C. Dorronsoro, S. Barbero, L. Llorente, and S. Marcos, "Detailed on-eye measurement of optical performance of rigid gas permeable contact lenses based on ocular and corneal aberrometry," *Optom. Vision Sci.* **80**, 115–125 (2003).
 25. S. Marcos, S. Barbero, L. Llorente, and J. Merayo-Llodes, "Optical response to myopic LASIK surgery from total and corneal aberration measurements," *Invest. Ophthalmol. Visual Sci.* **42**, 3349–3356 (2001).
 26. J. McLellan, S. Marcos, and S. A. Burns, "Age-related changes in monochromatic wave aberrations of the human eye," *Invest. Ophthalmol. Visual Sci.* **42**, 1390–1395 (2001).
 27. A. Guirao, M. Redondo, and P. Artal, "Optical aberrations of the human cornea as a function of age," *J. Opt. Soc. Am. A* **17**, 1697–1702 (2000).
 28. A. Glasser and M. Campbell, "Presbyopia and the optical changes in the human crystalline lens with age," *Vision Res.* **38**, 209–229 (1998).
 29. G. Smith, M. J. Cox, R. Calver, and L. F. Garner, "The spherical aberration of the crystalline lens of the human eye," *Vision Res.* **41**, 235–243 (2001).
 30. E. Moreno-Barriuso, S. Marcos, R. Navarro, and S. Burns, "Comparing laser ray tracing, spatially resolved refractometer and Hartmann-Shack sensor to measure the ocular wave aberration," *Optom. Vision Sci.* **78**, 152–156 (2001).
 31. R. Navarro and M. A. Losada, "Aberrations and relative efficiency of light pencils in the living human eye," *Optom. Vision Sci.* **74**, 540–547 (1997).
 32. L. N. Thibos, R. A. Applegate, J. T. Schwiegerling, R. Webb, and V. S. T. Members, "Standards for reporting the optical aberrations of eyes," in *Vision Science and Its Applications*, V. Lakshimarayanan, ed., Vol. 35 of OSA Trends in Optics and Photonics Series (Optical Society of America, Washington, D.C., 2000), pp. 110–130.
 33. L. Llorente, L. Diaz-Santana, D. Lara-Saucedo, and S. Marcos, "Aberrations of the human eye in visible and near infrared illumination," *Optom. Vision Sci.* **80**, 26–35 (2003).
 34. Z-136.1-1993, American National Standards Institute, "American national standard for the safe use of lasers" (The Laser Institute of America, Orlando, Fla., 1993).
 35. S. Barbero, S. Marcos, and J. Merayo-Llodes, "Corneal and total aberrations in a unilateral aphakic patient," *J. Cataract Refract. Surg.* **28**, 1594–1600 (2002).
 36. A. Guirao and P. Artal, "Corneal wave aberration from videokeratography: accuracy and limitations of the procedure," *J. Opt. Soc. Am. A* **17**, 955–965 (2000).
 37. M. J. Simpson, "Diffractive multifocal intraocular lens image quality," *Appl. Opt.* **31**, 3621–3626 (1992).
 38. M. Herzberger, "Colour correction in optical systems and a new dispersion formula," *Opt. Acta* **6**, 197–215 (1959).
 39. M. Dubbelman, H. A. Weeber, R. G. Van der Heijde, and H. J. Volker-Dieben, "Radius and asphericity of the posterior corneal surface determined by corrected Scheimpflug photography," *Acta Ophthalmol. Scand.* **80**, 379–383 (2002).
 40. P. Artal, E. Berrio, A. Guirao, and P. Piers, "Contribution of the cornea and internal surfaces to the change of ocular aberrations with age," *J. Opt. Soc. Am. A* **19**, 137–143 (2002).
 41. P. Waard, J. Jspeert, T. Van de Berg, and P. Jong, "Intraocular light scattering in age-related cataracts," *Invest. Ophthalmol. Visual Sci.* **33**, 618–625 (1992).
 42. P. Philips, H. Rosskothien, J. Emmanuelli, and C. Koester, "Measurement of intraocular lens decentration and tilt *in vivo*," *J. Cataract Refract. Surg.* **14**, 129–135 (1988).
 43. G. Smith and B. K. Pierscionek, "The optical structure of the lens and its contribution to the refractive status of the eye," *Ophthalmic Physiol. Opt.* **18**, 21–29 (1997).
 44. Y. Matsumoto, T. Hara, K. Chiba, and M. Chikuda, "Optimal incision sites to obtain an astigmatism-free cornea after cataract surgery with a 3.2 mm sutureless incision," *J. Cataract Refract. Surg.* **27**, 1615–1619 (2001).
 45. F. Mutlu, A. Bilge, H. Altinsoy, and E. Yumusak, "The role of capsulotomy and intraocular lens type on tilt and decentration of polymethylmethacrylate and foldable acrylic lenses," *Ophthalmologica* **212**, 359–363 (1998).
 46. C. K. Jung, S. K. Chung, and N. H. Baek, "Decentration and tilt: silicone multifocal versus acrylic soft intraocular lenses," *J. Cataract Refract. Surg.* **26**, 582–585 (2000).
 47. M. Wang, L. Woung, C. Hu, and H. Kuo, "Position of poly(methyl methacrylate) and silicone intraocular lenses after phacoemulsification," *J. Cataract Refract. Surg.* **24**, 1652–1657 (1998).
 48. A. Glasser and M. Campbell, "Biometric, optical and physical changes in the isolated human crystalline lens with age in relation to presbyopia," *Vision Res.* **39**, 1991–2015 (1999).
 49. T. Oshika and Y. Shiokawa, "Effect of folding on the optical quality of soft acrylic intraocular lenses," *J. Cataract Refract. Surg.* **22**, 1360–1364 (1996).